Collective excitations in x-ray spectra of metals*

G. D. Mahan
Physics Department, Indiana University, Bloomington, Indiana 47401
(Recived 14 January 1974)

New analytical and numerical results are presented for the many-body theory of x-ray spectra of metals. A method is presented whereby the previous edge theory is extended to the entire spectrum. It is shown that collective excitations do influence the entire spectrum, and not just the edge. Numerical results are presented for Li, Na, Mg, and Al, and compared to experiment. This theory is able to explain the $L_{2,3}$ absorption-edge shape, and the entire emission spectrum of lithium.

I. INTRODUCTION

The absorption of x rays in metals occurs by lifting an electron from an atomic-core state to the conduction band of the metals. This measurement provides direct information about electron energy bands in metals, and at one time was thought to directly measure the density of states.[1] Recently it has been realized that matrix elements change the spectra from a pure density-of-states measurement.[2-5]

Another recent development has been the appreciation of the role of many-body effects in influencing the x-ray spectra, in both absorption and emission.[6-9] Some time ago I suggested that exciton effects could alter the absorption and emission edge, and predicted a power-law dependence of absorption near threshold.[6] This suggestion was improved by Nozières and De Dominicis, who derived that the threshold behavior had the form[8]

$$A(\omega) = M_{l-1}^2 \left(\frac{\xi_0}{\omega - \omega_T}\right)^{\alpha_{l-1}} + M_{l+1}^2 \left(\frac{\xi_0}{\omega - \omega_T}\right)^{\alpha_{l+1}}, \tag{1.1}$$

$$\alpha_l = \frac{2\delta_l}{\pi} - 2\sum_{l'} (2l'+1)(\delta_{l'}/\pi)^2, \tag{1.2a}$$

$$g = 2\sum_{l'} (2l'+1)(\delta_{l'}/\pi)^2, \tag{1.2b}$$

where ξ_0 is a typical bandwidth, ω_T is the threshold frequency, $M_{l\pm1}^2$ are the intensities of the $l \pm 1$ partial wave, and the phase shifts are evaluated for the scattering of a conduction electron at the Fermi surface from the hole in the atomic core. This formula is asymptotically correct when $\omega - \omega_T \ll \xi_0$.

One difficulty with this expression is that it cannot be used away from threshold, since it predicts nonsensical results at large values of ω. One of the main results of the present analysis is to derive a way of overcoming this difficulty. We present an approximate calculation of the many-body effects at all absorption and emission frequencies. This gives (1.1) near threshold, but joins smoothly onto the other parts of the spectrum elsewhere. One important fact that has emerged from this analysis is that these collective excitation effects affect the entire spectrum, and not just near threshold.

We also present detailed numerical calculations for Li, Na, Mg, and Al. An attempt has been made to compute from first principles, and without adjustable parameters, the various parameters ξ_0, M_l, δ_l, etc. By and large they give a very good fit to the experimental spectra. The lack of knowledge of other key parameters, especially the x-ray level width from Auger transitions, prevents the attainment of perfect fits in all cases. However, the fits are good enough so that probably no other significant many-body processes are occurring.

Recently Dow and collaborators have suggested that the present theory does not explain the experimental data.[10-12] Our analysis does not support their assertion. Indeed, we even disagree with their numerical fits, as we get good agreement with calculated parameters quite different from those they get by fitting data. We conclude that their analysis is too naive, in that they make assumptions about the values of parameters, and these assumptions are untrue. Most of their conclusions, both numerical and analytical, can be disregarded. We have already shown that their phonon theory contains numerous difficulties.[13]

The previous theories of the threshold effects have been obtained by solving a model Hamiltonian which is called the "x-ray edge problem." In x-ray absorption, an electron is removed from the inner shell of an atom and put into a conduction-band state—thereby creating a hole in the atomic state. The model Hamiltonian includes the interaction between the conduction electrons and this x-ray hole state. The solution to this model Hamiltonian yielded the asymptotic formulas (1.1) in the threshold region. We give an approximate solution of the model Hamiltonian which yields (1.1) in the threshold region, but can be applied throughout the spectrum. It is essentially a convolution theory.

This model Hamiltonian does not include the interaction between conduction electrons, and thereby omits many physical processes. For example,

plasmon effects are omitted. But these excitations have sufficient energy so that they do not affect shapes of thresholds, nor even of main emission bands. Plasmon satellites are weak in emission, and not even positively identified in absorption. Omission of plasmon effects appears to this author to be a satisfactory approximation.

Another consequence of omitting electron-electron interactions is that one omits correlations in the electron gas. Flynn[12] has recently suggested that such correlations should be of great consequence. But the most exhaustive numerical treatment so far is by Bergersen, Brouers, and Longe,[13] who concluded that such correlation effects were not important. Their treatment, which proceeded by perturbation theory but kept all diagrams of first order, produced the edge singularity and Auger tail, but electron-gas effects seemed to have little other influence on the emission spectra they computed. Both the edge singularity and Auger tail are included in the present theory.

In the present analysis, we solve much more accurately the model Hamiltonian which was previously solved just for the threshold region. This theory reproduces quite well the two prominent features of the emission-spectrum-edge shapes and Auger tail. In absorption spectra, its applicability is probably limited to the threshold region, which is the only place where we use it.

Section II contains a detailed derivation of the method whereby the collective excitations can be extended to the entire spectrum. However, the same results can be derived by some simple arguments and sum rules. From the Kubo formula, one knows that the absorption spectra can be represented as the Fourier transform of a time-correlation function

$$A(\omega)=\int_{-\infty}^{\infty} dt\, e^{i\omega t} H^{(0)}(t) B(t),$$

where $H^{(0)}(t)$ is the Fourier transform of the ordinary spectra—from matrix elements and band structure—and $B(t)$ contains the effects of the many-body processes. The fact that $B(t)$ enters as a multiplication factor was shown by Nozières and De Dominicis.[8] Obviously the spectra can also be given by convolution in frequency space

$$A(\omega)=\int_{-\infty}^{\infty} d\omega' H^{(0)}(\omega-\omega') B(\omega').$$

The many-body effects enter through a factor $B(\omega)$. This has the effect of a broadening function, in that it tends to distort the features of the original spectra $H^{(0)}(\omega)$. This occurs not only at threshold, but throughout the spectra. The many-body effects are not just a feature at threshold, but affect the entire spectrum.

We show that it is a good approximation to express $B(\omega')$ as the product of two factors:

$$B(\omega')=C(\omega')D(\omega').$$

The first factor $C(\omega')$ is due to the excitonic interactions between the additional conduction electron, created in the absorptive process, and the x-ray hole. Pardee and Mahan[14] showed that the important factor in this term is

$$C(\omega')=C_0(\xi_0/\omega)^{2\delta_l(\omega)/\pi},$$

where C_0 is a normalization constant which will be specified below. The other factor $D(\omega')$, first discussed by Anderson,[7] is due to the excitations of the electron gas caused by the adjustment of the other conduction electrons to the hole in the x-ray level. We show in Sec. II that this term is accurately given by

$$D(\omega)=\frac{\Theta(\omega)}{\Gamma(g)\omega}\left(\frac{\omega}{\xi_0}\right)^{g} e^{-\omega/\xi_0},$$

$$g=\frac{2}{\pi^2}\sum_l (2l+1)\,\delta_l^2(k_F),$$

where the normalization constants make $D(\omega)$ integrable.

$$1=\int_{-\infty}^{\infty} d\omega\, D(\omega).$$

The broadening function $B(\omega)$ also must integrate to unity, since one can show that $B(t=0)=1$. This restriction serves to determine the constant C_0 above.

It is more convenient to do calculations with the exponent $2\delta_l/\pi$ in $C(\omega)$ treated as a constant $2\delta_l(k_F)/\pi$. This approximation was made in the present computations. This will have little effect upon the theoretical spectra calculated at threshold, which is of present concern. This is because the threshold is only a narrow energy region, while the phase shifts vary slowly with energy, as we will show by numerical computation. However, the correct broadening function, with a frequency-dependent phase shift, should probably be used for fitting spectra at a wide range of frequencies. Treating δ_l as a constant yields a simple formula for the normalization constant

$$B(\omega)=\frac{\Theta(\omega)}{\Gamma(-\alpha)\omega}\left(\frac{\xi_0}{\omega}\right)^{\alpha} e^{-\omega/\xi_0}.$$

A similar analysis of the emission spectra shows that it is also given by a convolution integral

$$I(\omega)=\int_{-\infty}^{\infty} d\omega' H^{(0)}(\omega+\omega') B(\omega'). \tag{1.3}$$

As an example, consider the emission from a conduction band to an s-state hole, as in K emission. The ordinary spectra have the form

$$H^{(0)}(\omega)=\omega^{3/2}\Theta(\omega)\Theta(E_k-\omega)$$

where we have omitted a very slowly varying func-

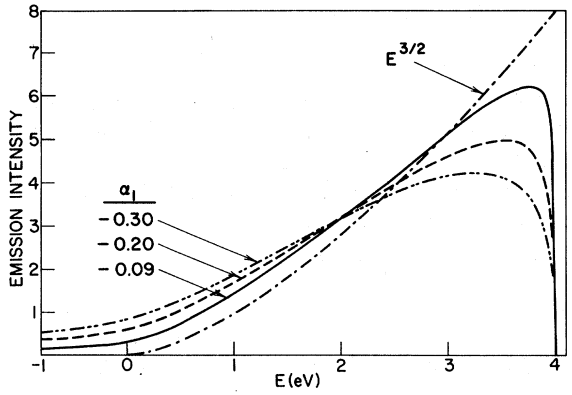

FIG. 1. Theoretical emission spectra for K shells, for different values of the edge parameter. The many-body effects of the present theory cause a round edge at threshold and a low-energy tail.

tion of ω which arises from the matrix element. The emission spectra (1.3) are shown in Fig. 1 for several values of α, and with $\xi_0 = E_F = 4.0$ eV. There are two important features of the calculated spectrum. The first is the threshold region near $\hbar\omega = E_F$. This has the rounded edge as expected from (1.1). The second region is the low-energy tail $\hbar\omega < 0$. This tail is observed in the experimental spectra, and was explained years ago by Landsberg[15-17] as being caused by Auger processes which accompany the x-ray transition. This is correct, and is exactly the same process which is being computed here. As noted by the Schottes,[18] the many-body processes which determine the threshold behavior are just Auger processes; so we expect that our theory, which describes the Auger and exciton processes throughout the emission band, should give the correct tail behavior which is caused by the Auger effect. It is evident that the broadening function $B(\omega)$ does affect the entire spectrum, and not just the threshold region. An important feature of the present theory is that we can calculate the entire spectrum and match it to experiment, rather than only to one spectral feature such as the threshold or the tail. It is immediately apparent that some earlier fits to experimental data are not correct. For example, Yue and Doniach[19] fit the threshold region of lithium and deduced that $\alpha_1 = -0.30$. Yet if the whole theoretical spectrum is calculated as in Fig. 1 and compared to the experiments, this high value of α_1 gives a very bad fit to the other parts of the spectrum. A much better fit to the whole spectrum is obtained from $\alpha_1 = -0.10$ which was calculated earlier.[5,20] The lithium spectrum is discussed much more extensively in Sec. III.

The phase shifts δ_l where $l = 0, 1, 2$, for Li, Na, Mg, and Al were calculated, and the results are shown in Figs. 2 and 3. The numerical details are explained in the Appendix, but basically a model potential was constructed from atomic data for each

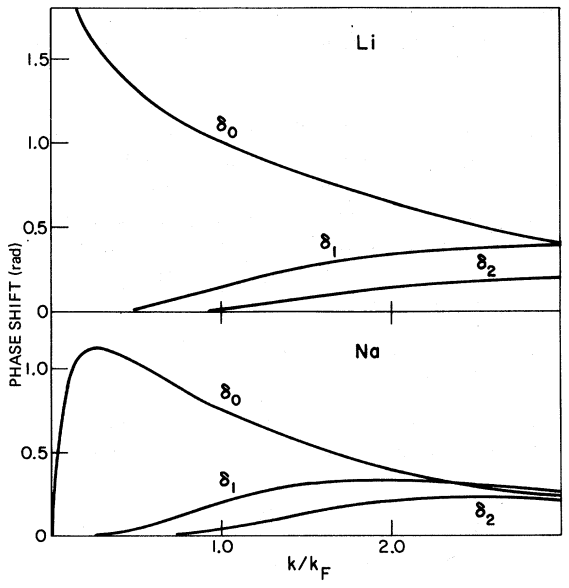

FIG. 2. Phase shifts for scattering of the conduction electron of wave vector k from the x-ray hole in lithium and sodium. The potentials are described in the Appendix. The lithium s-wave phase shift goes to the value of π at $k = 0$, indicating a bound state in the potential.

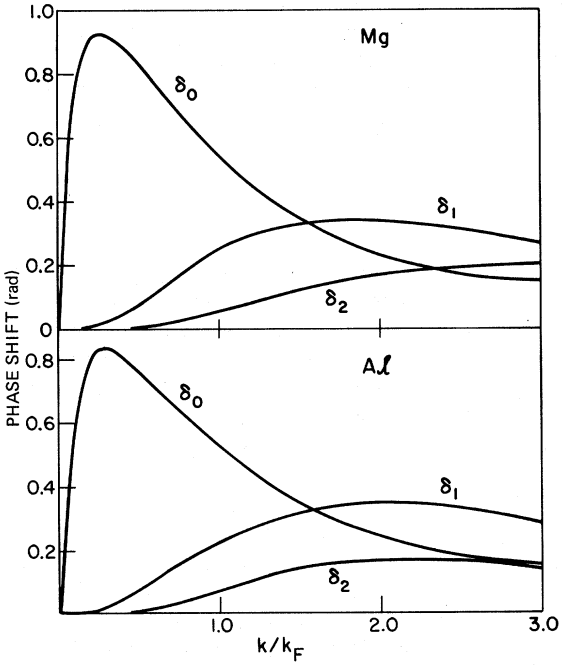

FIG. 3. Phase shifts for scattering of the conduction electron of wave vector k from the x-ray hole in magnesium and aluminum. The potentials are described in the Appendix.

TABLE I. Phase shifts and exponential factors which have been calculated by the methods in the Appendix. α_l and g are defined in Eqs. (1.2).

	Li	Na	Mg	Al
δ_0	1.02	0.76	0.55	0.53
δ_1	0.14	0.20	0.25	0.23
δ_2	0.025	0.042	0.056	0.073
g	0.22	0.14	0.101	0.09
α_0	0.42	0.34	0.25	0.24
α_1	−0.13	−0.02	0.06	0.05
α_2	−0.21	−0.12	−0.07	−0.05

ion (screened), and the phase shifts were computed by numerical solution. The phase shifts obey the Friedel sum rule. The variation of phase shift with wave vector is qualitatively similar to those calculated earlier for a screened point charge.[5] The values at the Fermi energy are shown in Table I.

II. IMPROVED EXCITATION THEORY

Nozières and De Dominicis[8] showed that the correlation function describing the collective excitations could be evaluated by solving for the time response. They obtained an approximate solution to the equations of this time function. Their solution was just valid in the threshold region. Here we wish to present an improved solution to the same equations. An approximate, simple, yet accurate solution is obtained which is valid throughout the spectrum.

First consider the hole Green's function of time in the Matsubara representation:

$$D(\tau) = -\langle T_\tau d(\tau) d^\dagger(0)\rangle$$

which they showed may be written as

$$D(\tau) = -\Theta(\tau) e^{-\epsilon_0 \tau} \langle S(\tau)\rangle ,$$

$$S(\tau) = T_\tau \exp \int_0^\tau d\tau' V(\tau') ,$$

where V is the electron-hole potential, which arises from the x-ray excited core level. By expanding the S matrix, it is easy to show that this correlation function can be evaluated by a linked-cluster theorem,[9] and the result is an exponential function of time

$$\langle S(\tau)\rangle = e^{-F(\tau)} . \tag{2.1}$$

The function $F(\tau)$ is a series of terms in increasing powers of the potential

$$F(\tau) = \tau N_0 V(0) + \frac{2}{2}\int_0^\tau d\tau_1 \int_0^\tau d\tau_2 \sum_{12} V_{12}V_{21}G_1(\tau_1-\tau_2)G(\tau_2-\tau_1)$$
$$+ \frac{2}{3}\int_0^\tau d\tau_1 \int_0^\tau d\tau_2 \int_0^\tau d\tau_3 \sum_{123} V_{12}V_{23}V_{31}G_1(\tau_1-\tau_2)G_2(\tau_2-\tau_3)G_3(\tau_3-\tau_1) + \tfrac{1}{2}\cdots \tag{2.2}$$

The factor of 2 is for spin. The subscripts 1, 2, 3, etc. refer to wave vectors—e.g., the potential is

$$V_{ij} = \int d^3r\, e^{-i(\vec{k}_i-\vec{k}_j)\cdot\vec{r}}\, V(r) ,$$

and the conduction-electron Green's function is

$$G_i(\tau) = -e^{-\tau\epsilon(k_i)}[\Theta(\tau) - N_{k_i}] .$$

The second and third term in the series (2.2) for $F(\tau)$ are

$$F_2(\tau) = 2\sum_{12} |V_{12}|^2 \left[\frac{-\tau N_1}{\xi_{21}} + \frac{N_1(1-N_2)}{(\xi_{21})^2}(1-e^{-\tau\xi_{21}})\right],$$

$$F_3(\tau) = 2\sum_{123}\left[V_{12}V_{23}V_{31}\frac{-\tau N_1}{\xi_{31}\xi_{21}} + \frac{N_1(1-N_2)(1-e^{-\tau\xi_{21}})}{\xi_{12}^2\xi_{23}}\right]$$
$$\times (V_{12}V_{23}V_{31} + V_{13}V_{32}V_{21}) + V_{12}V_{23}V_{31}$$
$$\times \frac{N_1N_2(1-N_3)}{\xi_{12}\xi_{23}\xi_{31}}(e^{-\tau\xi_{32}} - e^{-\tau\xi_{31}}) .$$

In each set of brackets the first term contributes to the self-energy, while the second term contributes to the excitation function of interest. These terms appear to be the series expansion for the T matrix.[21] So the contribution has the form

$$m(\tau) = 2\sum_{12} |T_{12}|^2 \frac{N_1(1-N_2)}{\xi_{21}^2}(1-e^{-\tau\xi_{21}}) . \tag{2.3}$$

At large τ this function asymptotically approaches

$$\lim_{\tau\to\infty} m(\tau) = (2/\pi^2)\ln(\tau)\sum_l (2l+1)\sin^2\delta_l .$$

If we presume that the other third-order term is just the first term in the expansion for

$$2\sum_{123} T_{12}T_{23}T_{31}\frac{N_1N_2(1-N_3)}{\xi_{12}\xi_{23}\xi_{31}}(e^{-\tau\xi_{32}} - e^{-\tau\xi_{31}})$$

then at large τ, this results in

$$(2/3\pi^2)\ln(\tau)\sum_l (2l+1)\sin^3\delta_l .$$

Thus we have generated the first two terms in the series

$$(2/\pi^2)\ln(\tau)\sum_l (2l+1)[\sin^2\delta_l + \tfrac{1}{3}\sin^3\delta_l + \cdots$$
$$= \text{arc}\sin^2(\sin\delta_l) = \delta_l^2]$$

which gives the δ_l^2 result of Nozières and De Domi-

nicis. We have also evaluated the lengthy fourth-order term, and ascertained that it does contain the next terms in the series for the T matrix.

We expect that $m(\tau)$ is the most important term among those contributing to the excitation spectra. Since most of the phase shifts are not large, and $\sin\delta \cong \delta$ for small phase shifts, this is certainly the dominant term at threshold. We assume, without proof, that it is dominant at all frequencies. Equation (2.3) for $m(\tau)$ may be rewritten as

$$m(\tau) = \int_0^\infty \frac{d\epsilon}{\epsilon}\rho(\epsilon)(1 - e^{-\epsilon\tau}), \tag{2.4}$$

$$\rho(\epsilon) = \frac{2}{\epsilon(2\pi)^6}\int d^3k_1 \int d^3k_2 N_1(1-N_2) \times \delta(\epsilon - \epsilon(k_2) + \epsilon(k_1))\left|T_{k_1k_2}\right|^2 . \tag{2.5}$$

The function $\rho(\epsilon)$ has been evaluated numerically for the four metals Li, Na, Mg, and Al. Using the methods described in the Appendix, the off-diagonal T matrix was calculated for conduction-electron scattering from the x-ray hole in the metal ion, and (2.5) was evaluated assuming free-electron gas values for $\epsilon(k)$ and N_k. The results are shown in Fig. 4, plotted in reduced units. Of course

$$g = \rho(0) = \frac{2}{\pi^2}\sum_l (2l+1)\sin^2\delta_l .$$

The curves for Mg and Al coincide, and are very similar to those for Li and Na. Also shown are two exponential functions $e^{-\epsilon/\xi_0}$ for $\xi_0 = E_F$ and $\frac{3}{2}E_F$.

The reason that the exponential fit is interesting is that if we set

$$\rho(\epsilon) = ge^{-\epsilon/\xi_0}, \tag{2.6}$$

then (2.4) may be integrated exactly to give

$$m(\tau) = g\int_0^\infty \frac{d\epsilon}{\epsilon} e^{-\epsilon/\xi_0}(1 - e^{-\tau\epsilon}) = g\ln(1+\tau\xi_0)$$

The effect upon a spectral shape is determined by

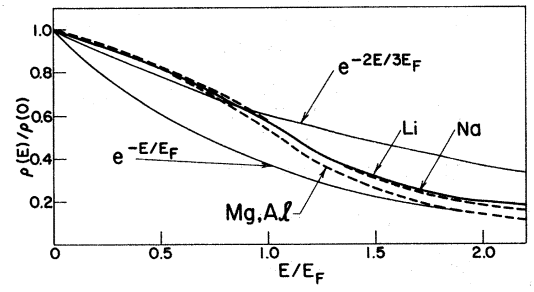

FIG. 4. A plot of $\rho(\epsilon)$ vs E/E_F for Li, Na, Mg, and Al. This function is defined in Eq. (2.5), and describes the strength of excitations of the electron gas. The curves for Mg and Al coincide, and those for Li and Na nearly do also. Two exponentials are also shown, with widths E_F and $\frac{3}{2}E_F$.

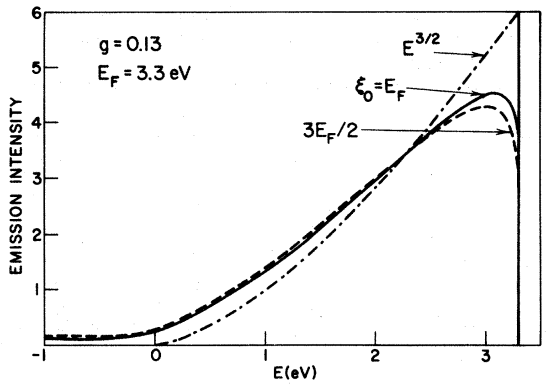

FIG. 5. Effects of different widths upon the K-shell emission spectrum.

changing $\tau \to it$, and performing the necessary time integral. For a δ-function line, this is

$$B(\omega) = \int_{-\infty}^{\infty}\frac{dt}{2\pi}\, e^{i\omega t}e^{-g\ln(1+it\xi_0)}$$

which may be exactly evaluated to give

$$B(\omega) = \frac{\Theta(\omega)}{\Gamma(g)\omega}\left(\frac{\omega}{\xi_0}\right)^g e^{-\omega/\xi_0}, \tag{2.7}$$

where Γ is a gamma function and Θ is the step function. Furthermore, other absorption spectra

$$A(\omega) = \int_{-\infty}^{\infty} dt\, H(\tau)\, e^{i\omega t}\, e^{-g\ln(1+it\xi_0)}$$

can be evaluated by convolution

$$A(\omega) = \int_{-\infty}^{\infty} d\omega' H(\omega - \omega')B(\omega'), \tag{2.8}$$

where $H(\omega)$ is the absorption spectra in the absence of excitations. This is a rather simple result. It says that the effects of the excitations of the electron gas can be included by just convoluting the ordinary spectra with the broadening function $B(\omega)$. The ordinary spectra would include the effects of matrix elements and density of states.

The broadening function we suggest in (2.7) is only rigorously correct if $\rho(\epsilon)$ is an exponential function. However, the function $B(\omega)$ has two features which are necessary in the correct broadening function. First, it has the power-law behavior ω^g which is asymptotically correct, and secondly it is integrable

$$1 = \int_{-\infty}^{\infty} d\omega\, B(\omega) .$$

This ensures the f-sum rule—that the broadening function does not change the net oscillator strength. We propose this form of the broadening function as a simple and useful method of incorporating the effects of collective excitations into theoretical spectra.

The width ξ_0 should be chosen to be somewhere between E_F and $\frac{3}{2}E_F$. The difference between these choices is less than one might think. Figure 5 shows a calculated emission spectrum where $B(\omega)$ has been convoluted with $\omega^{3/2}$ for $\xi_0 = E_F$ and $\xi_0 = \frac{3}{2}E_F$. The bandwidth 3.3 eV and $g = 0.13$ were those expected for lithium. The two curves almost coincide, except in the threshold region. They do, in fact, coincide if one treats them as in a fitting procedure—namely, shift one with respect to the other in energy so that their peaks coincide, and then rescale intensities so that the peak heights are equal. Then they differ only in the threshold region, as is expected for a simple $[(\omega - \omega_T)/\xi_0]^g$ behavior. We concluded that the spectrum does not depend sensitively upon the choice of the parameter ξ_0.

The hole Green's function is an important factor in determining the spectra. Another important many-body term is the exciton effect caused by introducing the extra electron to the conduction band. To evaluate this contribution, we follow our previous analysis[9] and evaluate the correlation function

$$A_j(t) = \frac{-i}{\Omega}\sum_{kk'} W_j(\vec{k})W_j(\vec{k}')\langle| d_j(t)C_{\vec{k}'}(t)C^{\dagger}_{\vec{k}}(0)d^{\dagger}_j(0)|\rangle ,$$

where $W_j(\vec{k})$ are just the dipole matrix elements for the interband transition from the core level j to the conduction-band state $\vec{k}$

$$W_j(\vec{k}) = \int d^3r\, \Psi_{\vec{k}}(r)\,\vec{\hat{\epsilon}}\cdot\vec{p}\,\Phi_j(r)$$

and d_j and c_k are the destruction operators of the hole and conduction electron. The S matrix is expanded, and collected into an exponential series, with the result

$$\begin{aligned} A_j(t) &= -i\Theta(t)\, e^{-it(\epsilon_j+\mu)}\sum_{lm} H^{(0)}_{lmj}(t)\, e^{M_{lmj}(t)}, \\ M_{lmj}(t) &= -F(t) + N_{lmj}(t), \end{aligned} \tag{2.9}$$

where (l, m) are the angular quantum numbers of the conduction electron. The exponent contains the hole term $F(t)$ in (2.2) and the exciton term $N_{lmj}(t)$. An examination of the series expansion for N_{lmj} shows that its leading term $N^{(1)}_{lmj}$

$$\begin{aligned} N^{(1)} &= H^{(1)}_{lmj}/H^{(0)}_{lmj}, \\ H^{(1)}_{lmj} &= \frac{4\pi\times 2}{(2\pi)^6}\int d^3k \int d^3k'\, w_{lmj}(k)w_{lmj}(k') \\ &\quad\times(1-N_k)(1-N_{k'})\frac{e^{-it\xi_{k'}}}{\xi_{k'}-\xi_k}\, T_l(k, k'), \\ T_{kk'} &= 4\pi\sum_l (2l+1)P_l(\hat{k}\cdot\hat{k}')T_l(k, k'), \end{aligned} \tag{2.10}$$

where $H^{(0)}_{lmj}$ is the correlation function for the ordinary spectra (without collective effects)

$$H^{(0)}_{lmj}(t) = \int \frac{d^3k}{(2\pi)^3}\,|w_{lmj}(k)|^2 e^{it\xi_k t}(1-n_k),$$

$$W_j(k) = (4\pi)^{1/2}\sum_{lm} w_{lmj}(k)Y^m_l(\hat{k}\cdot\hat{\epsilon}).$$

Again these integrals are done easily if an exponential form is assumed for the matrix elements:

$$H^{(0)} = w_0^2 N_F \int_0^{\infty} d\epsilon\, e^{-i\epsilon t}\, e^{-\epsilon/\epsilon_1},$$

$$H^{(1)} = 8\pi w_0^2 N_F^2 T_l(k_F, k_F)\int_0^{\infty} d\epsilon\, e^{-it\epsilon}\, e^{-\epsilon/\epsilon_2} \times\int_0^{\infty}\frac{d\epsilon'\, e^{-\epsilon/\epsilon_2}}{\epsilon-\epsilon'}$$

gives

$$H^{(0)} = \frac{w_0^2 N_F \epsilon_1}{1+it\epsilon_1}$$

$$H^{(1)} = 8\pi w_0^2 N_F^2 T_l \frac{\epsilon_2}{1+it\epsilon_2}\ln(1+2it\epsilon_2),$$

where

$$8\pi N_F T_l = (2/\pi)\sin\delta_l .$$

This gives for the form of the exponential function

$$N^{(1)} = \frac{2}{\pi}\sin\delta_l \frac{\epsilon_2}{\epsilon_1}\frac{1+it\epsilon_1}{1-it\epsilon_2}\ln(1+2it\epsilon_2). \tag{2.11}$$

The most convenient assumption is to set

$$\epsilon_1 = \epsilon_2 = \tfrac{1}{2}\xi_0$$

which would make the exciton term have the same time dependence as the hole term. This is most convenient numerically. Physically we expect $\epsilon_2 \approx \frac{1}{2}\xi_0$ to be nearly right, but not $\epsilon_1 \approx \epsilon_2$, since the parameter ϵ_1 is determined by the matrix-element dependence upon energy, while the others are dependent upon the T matrix. However, the approximation $\epsilon_1 \approx \epsilon_2$ does not change the behavior in the threshold region since at large time the expression (2.10) becomes independent of ϵ_1.

The result of this analysis is to suggest that a simple approximate form for the entire exponential part of the excitation function is

$$M_l = \alpha_l \ln(1+it\xi_0),$$

where α_l is the Nozières–De Dominicis exponent (1.2). As discussed in the introduction, it is more accurate to use the Pardee-Mahan result for the exciton contribution, but this is more cumbersome numerically. Our analysis only included the $\sin\delta_l$ terms, but these are the largest contributions to α_l. If $A_0(\omega)$ and $I_0(\omega)$ are the absorption and emission spectra in the absence of excitation effects, then excitation effects may be included by convolution

$$A(\omega) = \int_0^{\infty} d\omega' A_0(\omega-\omega')B(\omega'),$$

$$I(\omega) = \int_0^{\infty} d\omega' I_0(\omega+\omega')B(\omega'),$$

with the broadening function (2.7) obtained by setting $g=-\alpha_l$:

$$B(\omega)=\frac{\Theta(\omega)}{\Gamma(-\alpha)\omega}\left(\frac{\xi_0}{\omega}\right)^{\alpha} e^{-\omega/\xi_0}.$$

III. LITHIUM

Lithium is the metal whose x-ray spectrum is most often measured,[22,23] calculated,[24–26] and debated.[10] The reason is that the system is simple and should be easy to understand. The atomic core contains only one state, the $1s$, while the conduction band is thought to be nearly spherical and confined to one Brillouin zone of the metal.

The spectrum has been measured in both emission[22,23] and absorption.[27] The absorption data is of very high quality,[27] but it is difficult to analyze a whole spectrum because of energy-band effects. These enter the spectrum within a few electron volts of threshold, both theoretically[5] and experimentally.[27] A proper analysis would need to include all of these effects, which would increase the number of parameters that would have to be introduced to calculate the spectrum. Instead, it was decided to just analyze the emission data, which are free of these effects. The difficulty with the emission data is that there are experimental problems with self-absorption, and excitation effects with the result that different experimentalists often do not agree. Thus the experimental situation itself is uncertain. We have chosen, somewhat arbitrarily, to use Sagawa's data as the basis of our comparison.[23]

Figure 6 shows the comparison of our theory to the emission spectra of lithium. The theoretical spectrum was calculated with the parameters $E_F=3.3$ eV, $\xi_0=\frac{3}{2}E_F$, and $\alpha_1=-0.13$. The value of E_F was obtained from Ham,[28] and seems to fit the data, while the others were calculated using the methods already described. The calculated value of $\alpha_1=-0.13$ is not significantly different from the previous values $\alpha_1=-0.10$, nor is $\xi_0=\frac{3}{2}E_F$ significantly different from $\xi_0=E_F$. We calculated theoretical spectra with different combinations of these parameters, and none were very different from that of Fig. 6.

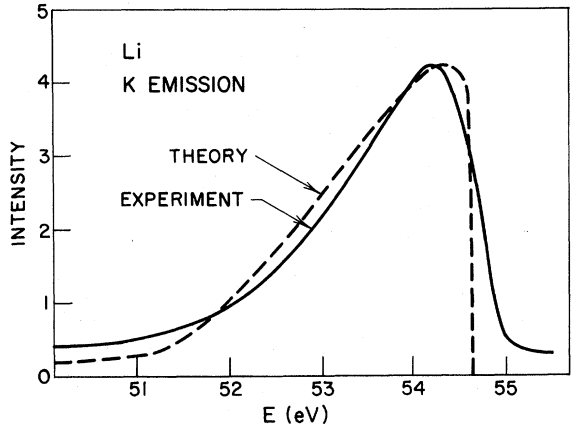

FIG. 6. A comparison between theory and experiment for the K-shell emission of lithium. The experimental threshold of 54.6 eV is much broader than the theory, which is probably because of the Auger width of the core hole level. There are no adjustable parameters in the theory, so the agreement with experiment is good. The experiments are from T. Sagawa in Ref. 23.

The theoretical spectrum is too low in the low-energy tail region. This is not significant. The entire emission spectrum is superimposed on a smooth background. We cannot compare the emission in this frequency region without knowledge of how this experimental background was subtracted. The present theoretical result, showing that the theory predicts a very flat, extended tail region, renders such subtractions suspect.

The interesting region to compare theory with experiment is in the threshold region near 54.6 eV. Here the theoretical curve falls off more sharply than does the experimental spectrum. The absorption spectrum has about the same threshold shape, albeit inverted, as does the emission spectrum. In this region the emission and absorption spectra overlap.

Our hypothesis is that the x-ray hole in lithium has a lifetime width of $\Gamma\simeq 0.2$–0.3 eV. This is sufficient to explain the discrepancy between the theoretical and experimental widths in both emission and absorption. It also explains the overlap between the emission and absorption. This lifetime is very likely caused by the Auger effect. The x-ray level width of metallic lithium has neither been measured nor calculated.

However, other evidence exists which shows that this is a reasonable hypothesis. Theoretical calculations of the K-shell level width in atomic Na, Mg, and Al produce numbers of exactly this magnitude—0.3 eV.[29] These calculations were not extended to lithium, but an extrapolation of their tables to the lithium atomic number produces the estimate of a zero level width. This is not surprising; in fact it is expected. It takes two upper-state electrons to have an Auger process, and *atomic* lithium does not have that many. Metallic lithium does, since all of the conduction electrons are available. We performed a quick and crude estimate of the Auger width in metallic lithium using orthogonalized plane waves (OPW), and came up with 0.2 eV. This appears to be a reasonable estimate.

Dow, Robinson, and Carver (DRC)[10] have suggested that the extra edge width in lithium arises from phonon broadening. We have shown elsewhere[11] that this suggestion encounters several dif-

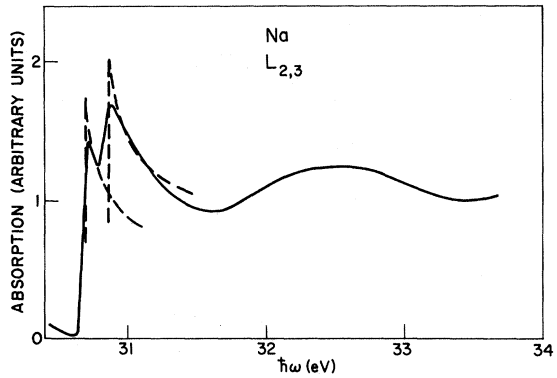

FIG. 7. A comparison of experiment (solid line) and theory (dashed line) for the $L_{2,3}$ absorption edge of sodium. The theory has no adjustable parameters, and so the fit is quite good. The agreement would be improved by adding the level width of the core hole, but unfortunately they are not known so they would have to be adjustable parameters. The fit to the L_3 absorption edge is excellent. The experiments are from Kunz *et al.* in Ref. 27.

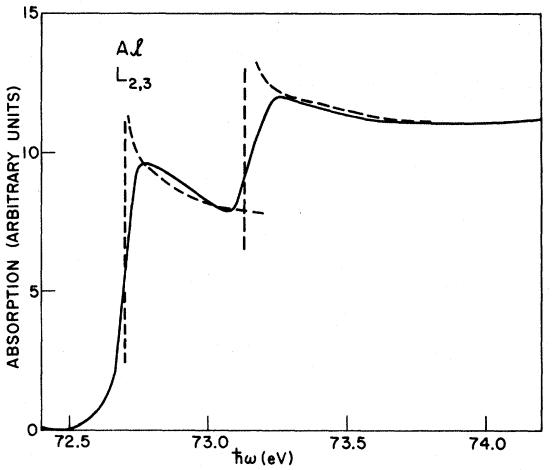

FIG. 9. A comparison of experiment (solid line) and theory (dashed line) for the $L_{2,3}$ absorption edge of aluminum. The theory has no adjustable parameters, and so the fit is quite good. The agreement would be improved by adding the level width of the core hole which unfortunately is not known. The experiments are from Kunz *et al.* in Ref. 27.

ficulties and must be discarded: First, it predicts the edge width is temperature dependent—which it is not, and second, it predicts an energy gap of 2 eV between the emission and absorption spectra, whereas in fact they overlap.

The theoretical curve in Fig. 6 was calculated just as in Fig. 1; it is a convolution of $\omega^{3/2}$ and $B(\omega)$. The many-body processes have a significant effect upon the spectra. They produce a pronounced broadening and rounding of the $\omega^{3/2}$ spectra, which is most evident in Fig. 1. This theory, along with the suggested level width, is sufficient to explain the experimental emission data.[30]

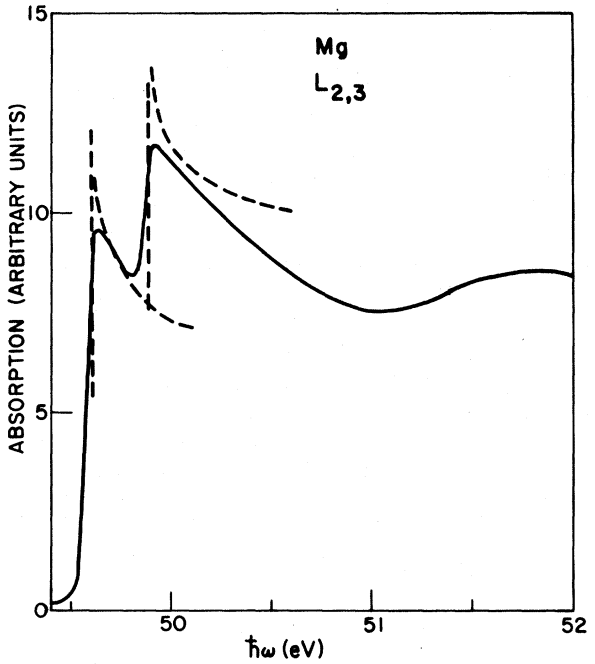

FIG. 8. A comparison of experiment (solid line) and theory (dashed line) for the $L_{2,3}$ absorption edge of magnesium. The theory has no adjustable parameters. The fit to the L_3 edge is good, but not to the L_2 edge. The experiments are from Kunz *et al.* in Ref. 27.

IV. $L_{2,3}$ EDGE IN Na, Mg, Al

Excellent experimental data exist for the $L_{2,3}$ absorption edge in sodium, magnesium, and aluminum.[27,31] Thus it is interesting to see how the theory explains the experimental spectra. These comparisons are shown in Figs. 7, 8, and 9. The theoretical spectrum was computed using (1.1) and the parameters in Tables I and II. The L_2 edge was added in with one-half of the intensity of the L_3 edge, with an energy separation given by the atomic spin-orbit interaction Δ. For a p-state hole, the two terms in (1.1) refer to s- and d-wave conduction band states. The s-wave part is a diverging threshold ($\alpha_0 > 0$), while the d-wave part is a converging threshold ($\alpha_2 < 0$).

The agreement between theory and experiment is rather good for Na and Al, and rather bad for Mg. In assessing the agreement between theory and experiment, one should consider the various parameters which enter into the theory. These are listed in Table III. The present analysis has attempted calculations on the last four of these. We set Γ_2 and Γ_3 equal to zero, and we took $E_{L3} - E_{L2}$ to be the atomic spin-orbit energy. Inspection of Figs. 7, 8, and 9 shows that this may not be cor-

rect, especially for aluminum. Two critical parameters for fitting purposes are the hole energy widths Γ_2 and Γ_3. They are different,

$$\Gamma_2 > \Gamma_3 ,$$

because the L_2 hole decays very rapidly into an L_3 hole by an Auger transition. Close inspection of the experimental data shows the L_2 edge to be wider than the L_3. Another problem with comparing theory to experiment is that the background absorption is not a constant as is assumed in the theory. This background has two sources: One is the band-structure effects in the $L_{2,3}$ edge itself, as is evident in sodium; the other is the background absorption which forms a continuum that varies with energy.

There are no adjustable parameters in the theory, except an arbitrary scale factor on intensity, which is necessary since absolute experimental numbers were not provided. Thus the perfect agreement with the sodium L_3 edge appears rather spectacular. Similarly, the entire aluminum spectra is a good fit, particularly the L_2 edge where the high-frequency falloff matches experiment exactly. We have no explanation as to why the Mg theory compares so unfavorably. The difficulty is that the L_2 and L_3 experimental edges do not seem to have the required 1 : 2 intensity ratios.

The most important parameter for calculating the theoretical spectra is the ratio $\mathcal{F}$ of d-wave to s-wave intensity. This quantity is calculated in the Appendix, following a method suggested in Ref. 32 with the results shown in Table II. The ratio changes rather drastically, from 0.5 for Na to 2.7 for Al. An independent calculation by Ritsko, Schnatterly, and Gibbons using slightly different wave functions obtains 2.0 for Al. This is satisfactory agreement with our theory, since the theory is sufficiently crude that these are almost estimates. If we use their ratio of $\mathcal{F} = 2$ for aluminum we fit the data about as well. The important message is that the aluminum $L_{2,3}$ edge is predominantly d wave. This explains why it *appears* less sharp than the Mg edge, which has almost the same values for α_0 and α_2.

TABLE II. Parameters which have been assumed or derived in the present analysis. All energies are in Rydberg units (13.6 eV.), and other units are also atomic. Many of these numbers are derived in the Appendix.

	Li	Na	Mg	Al
E_F	0.24	0.23	0.52	0.86
r_i	1.50	1.80	1.50	1.20
A_0	+0.86	+0.20	−0.04	+0.66
A_0'	−0.83	−0.87	−1.18	−0.94
A_1	−2.22	+0.15	−0.66	−0.82
A_1'	−4.08	−0.91	−2.28	−3.24
A_2	−2.62	−3.20	−4.64	−8.16
A_2'	−3.33	−3.34	−6.17	−9.35
k_s	0.89	0.84	0.92	1.05
E_{1s}		78.5	95.4	114.0
E_{2s}		4.64	5.23	7.81
E_{2p}		2.00	3.10	4.49
E_{s0}		0.0125	0.0206	0.0317
$\mathcal{F}$		0.48	1.64	2.68

TABLE III. Parameters which must be known or assumed in order to fit the $L_{2,3}$-absorption-edge spectra.

Symbol	Name	Restriction
E_{L3}	L_3-edge energy	$E_{L3} - E_{L2} \simeq \Delta$
E_{L2}	L_2-edge energy	
Γ_3	L_3-hole width	$\Gamma_2 > \Gamma_3$
Γ_2	L_2-hole width	
$\mathcal{F}$	Ratio of d to s wave	
ξ_0	Width of broadening function	$\xi_0 \simeq E_F$
α_0	s-wave exponent	
α_2	d-wave exponent	

Dow and Sonntag[10] have analyzed the $L_{2,3}$ edge, and concluded that the parameter α_0 varies considerably from metal to metal. They do not present the details of their analysis, but we judge it to be incorrect. Our first criticism is that the d-wave fraction of the edge absorption is changing significantly as r_s changes, which seems to be the predominant effect, rather than screening which they suggest. Since they do not mention the large change in d-wave fraction, we presume they overlooked it. Indeed, Dow in his Letter[10] assumes $\mathcal{F} = 0$ and ignores the d-wave contribution. This is a serious blunder which negates his analysis. Secondly, in past analyses[10] they have made the error of setting d-wave phase shifts equal to zero. We find that to be a significant error for aluminum, where the d waves contribute over 20% to the Friedel sum rule and change the value of α_2 by a factor of 2. The latter is very significant for fitting procedures, since the edge contains so much d wave. Indeed, from Table III one can see that they would need to fit seven other parameters in order to obtain the one they want, α_0. This seems to be a dubious procedure. Their conclusion—that the Nozières–De Dominicis theory does not explain the spectra—can be discarded. Indeed, we feel that the present calculations show that the theory is capable of explaining the experimental data very well.

APPENDIX: NUMERICAL METHODS

The important aspect of the numerical method is to obtain a potential which describes the scattering of an electron from the hole in the core state. This was done using the model potential of Heine-Abarankov.[33] This has the form for angular momentum

state l:

$$V(r)=A_l, \qquad r<r_i$$
$$V(r)=-2Z/r, \quad r>r_i \ ,$$

where atomic units are used throughout. The parameter r_i was chosen from Pauling's table of ionic radii.[34] A_l is obtained by fitting to atomic energy levels.[35] This is done for the normal metal ion of valence $Z=1, 2, 3$ for Na, Mg, Al—and also for the ion with a core hole and valence $Z+1$. The atomic values of A_l are extrapolated to the Fermi energy, which is taken as the negative of the work function.[36] The values of r_i, A_l, and A_l' are shown in Table II, where A_l' are the values for the ion with $Z+1$ valence. The electron-core hole potential was taken as the difference

$$V(r)=A_l'-A_l, \quad r<r_i$$
$$V(r)=-2/r, \quad r>r_i \ .$$

Thomas-Fermi screening was introduced by Fourier transforming this potential, dividing by $\epsilon(q)=1+k_s^2/q^2$, and Fourier transforming back to r space, with the result

$$V(r)=(-1/r)\{[(1-V_l)\,\mathrm{sgn}(r-r_i)+V_l/k_s r_i]e^{-k_s(r-r_i)} + (1-V_l-V_l/k_s r)e^{-k_s(r+r_i)}\} \ , \qquad \text{(A1)}$$
$$V_l=-\tfrac{1}{2}r_i A_l \ .$$

The screening constant k_s was determined by insisting that the phase shifts obey the Friedel sum rule

$$1=(2/\pi)\sum_l (2l+1)\delta_l(k_F) \ .$$

The phase shifts for $l=0, 1, 2$ are obtained by numerically integrating the radial part of Schrödinger's equation out from the origin using standard Runge-Kutta techniques.[37] At large values of r the wave function was fitted to the usual form

$$\Phi_l(k,r)=C[\cos\delta_l j_l(kr)+\sin\delta_l \eta_l(kr)]$$

which determined the phase shifts. These are plotted in Figs. 2 and 3, and the values at the Fermi surface are shown in Table I. Another definition of the phase shifts was considered. This is by separately calculating the phase shift for the screened model potential of the Z and the $Z+1$ valence ions, and then subtracting them. These numerical values were very similar to those presented here.

The T matrix in (2.5) was evaluated using the standard expansion (2.10), where the angular term is defined as[21]

$$T_l(k,k')=\int_0^\infty r^2 dr\, j_l(kr)V(r)\Phi_l(k',r) \ .$$

This was computed by direct numerical integration, using the screened model potential (A1) and its wave function $\Phi_l(k,r)$ which had been stored from the previous phase-shift calculation. The off-diagonal T-matrix terms $T_l(k,k')$ were computed and used in the calculation. A convenient check on numerical accuracy is obtained from the diagonal terms, which obey the relationship

$$T_l(k,k)=(1/2mk)\sin\delta_l(k) \ .$$

This value of phase shift agreed to about 1% with that obtained directly from the wave function.

Another numerical calculation was the ratio of d-wave to s-wave intensity in the $L_{2,3}$ absorption spectra. This was calculated assuming that the atomic orbitals were of the form

$$\Phi_{1s}(r)=[1/(\pi a_1^3)^{1/2}]e^{-r/a_1}$$
$$\Phi_{2p_z}=Ze^{-r/a_2}$$
$$\Phi_{2s}=[N/(\pi a_3^3)^{1/2}](1-\lambda r/3a_3)e^{-r/a_3}$$

while the conduction orbitals were an orthogonalized plane wave

$$\Psi_k(r)=e^{i\vec{k}\cdot\vec{r}}-\sum_\alpha |\alpha\rangle\langle\alpha|k\rangle \ .$$

λ was chosen so that $2s$ was orthogonal to $1s$, and N is a normalization constant

$$\lambda=1+a_3/a \ ,$$
$$N=(1-\lambda+\tfrac{1}{3}\lambda^2)^{-1/2} \ .$$

The atomic radii a_j were obtained from the observed eigenvalue

$$\epsilon_j=\hbar^2/2ma_j^2 \ ,$$

where ϵ_j is measured from the bottom of the conduction band. After sorting out the Clebsh-Gordan coefficients, we determine that the d- and s-wave matrix elements are proportional to

$$M_2=\frac{\sqrt{2}}{3}\int_0^\infty r^2 dr\, j_2(kr)\left(\frac{r}{a_2}\right)e^{-r/a_2} \ ,$$

$$M_0=\int_0^\infty r^2 dr\,\Phi_0(k,r)e^{-r/a_2}(1-r/3a_2) \ ,$$

where

$$\Phi_0=j_0(kr)-\frac{8e^{-r/a_1}}{(1+q_1^2)^2} - \frac{8N^2(1-\lambda r/3a_3)e^{-r/a_3}}{(1+q_3^2)^2}\left(1-\frac{\lambda(1-\frac{1}{3}a_3^2)}{1+q_3^2}\right)$$

and $q_j=ka_j$. These integrals give

$$M_2=\frac{8a_2^3}{3}\,\frac{\sqrt{2}q_2^2}{(1+q_2^2)^3} \ ,$$

$$M_0=\frac{8a_2^3}{3}\left(\frac{q_2^2}{(1+a_3^2)^2}-\frac{6a_2/a_1}{(1+q_1^2)^2(1+a_2/a_1)^4}\right.$$

$$-\frac{2\alpha}{(1+a_2/a_3)^5}\frac{a_2}{a_1a_3}(a_3+4a_1-3a_2)\Big) ,$$

$$\alpha=\frac{1+a_3^2-\lambda(1-\frac{1}{3}q_3^2)}{(1+q_3^2)^3(1-\lambda-\lambda^2/3)} ,$$

so the ratio $\mathcal{F}$ of d- to s-wave intensity is

$$\mathcal{F}=|M_2/M_0|^2 .$$

These results are also shown in Table II.

---

*Research supported by the National Science Foundation.

[1]D. H. Tomboulian, *Handbuch der Physik* (Springer, Berlin, 1957), Vol. 30, pp. 246–304.

[2]G. A. Rooke, in *Soft X-Ray Band Spectra*, edited by D. J. Fabian (Academic, New York, 1968), p. 3.

[3]W. A. Harrison, *ibid.*, p. 227.

[4]N. W. Ashcroft, *ibid.* p. 249.

[5]G. D. Mahan, J. Res. Natl. Bur. Stand. (U.S.) A 74, 267 (1970).

[6]G. D. Mahan, Phys. Rev. 163, 612 (1967).

[7]P. W. Anderson, Phys. Rev. Lett. 18, 1049 (1967).

[8]P. Nozières and C. T. De Dominicis, Phys. Rev. 178, 1097 (1969).

[9]G. D. Mahan, *Solid State Physics*, edited by H. Ehrenreich, F. Seitz, and D. Turnbull (Academic, New York, 1974), Vol. 29, pp. 75–138.

[10]J. D. Dow, J. E. Robinson, and T. R. Carver, Phys. Rev. Lett. 31, 759 (1973); J. D. Dow and D. L. Smith, J. Phys. F 3, L170 (1973); J. D. Dow and B. F. Sonntag, Phys. Rev. Lett. 31, 1461 (1973); J. D. Dow, Phys. Rev. Lett. 31, 1132 (1973).

[11]G. D. Mahan (unpublished).

[12]C. P. Flynn, Phys. Rev. Lett. 32, 1058 (1974).

[13]B. Bergersen, F. Brouers, and P. Longe, J. Phys. F 1, 945 (1971).

[14]W. J. Pardee and G. D. Mahan, Phys. Lett. 45A, 117 (1973).

[15]P. T. Landsberg, Proc. R. Soc. Lond. A62, 806 (1949).

[16]A. J. Glick and P. Longe, Phys. Rev. Lett. 15, 589 (1965).

[17]A. Morita and M. Watabe, J. Phys. Soc. Jpn. 25, 1060 (1968).

[18]K. D. Schotte and U. Schotte, Phys. Rev. 182, 479 (1969).

[19]J. T. Yue and S. Doniach, Phys. Rev. B 8, 4578 (1973).

[20]G. A. Ausman and A. J. Glick, Phys. Rev. 183, 687 (1969).

[21]L. I. Schiff, *Quantum Mechanics*, 3rd ed. (McGraw-Hill, New York, 1968), Sec. 37.

[22]R. S. Crisp and S. E. Williams, Philos. Mag. 5, 525 (1960).

[23]T. Sagawa, in Ref. 2, p. 29.

[24]F. K. Allotey, Phys. Rev. 157, 467 (1967); Solid State Commun. 9, 91 (1971).

[25]R. T. Shuey, Phys. Kondens. Materie 5, 192 (1966).

[26]M. J. Stott and N. H. March, in Ref. 2, p. 283; Phys. Lett. 23, 408 (1966).

[27]C. Kunz, R. Haensel, G. Keitel, P. Schreiber, and B. Sonntag, *Electronic Density of States*, edited by L. H. Bennett, Natl. Bur. Stand. Spec. Publ. 323 (U.S. G.P.O., Washington, D.C., 1971), p. 275.

[28]F. S. Ham, Phys. Rev. 128, 82 (1962); 128, 2524 (1962).

[29]W. Banbynek, B. Crasemann, R. W. Fink, H. U. Freund, H. Mark, C. D. Swift, R. E. Price, and P. Vengopala Rao, Rev. Mod. Phys. 44, 716 (1972).

[30]One difficulty with analyzing lithium is that the conduction-band effective mass is significantly different from unity. This is why the Fermi energy we use, 0.24, is different from the free-electron value. However, the phase shifts were computed assuming a free-electron mass, which may be a dubious procedure.

[31]C. Gahwiller and F. C. Brown, Phys. Rev. B 2, 1918 (1970).

[32]J. J. Ritsko, S. E. Schnatterly, and P. C. Gibbons, Phys. Rev. Lett. 32, 671 (1974).

[33]V. Heine and I. V. Abarenkov, Philos. Mag. 9, 451 (1964); 12, 529 (1965).

[34]L. Pauling, *The Nature of the Chemical Bond*, 3rd ed. (Cornell U.P., Ithaca, N.Y., 1960), p. 514.

[35]C. E. Moore, *Atomic Energy Levels*, Natl. Bur. Stand. Circ. 467 (U.S. G.P.O., Washington, D.C., 1949), Vol. I.

[36]V. S. Fomenko, *Handbook of Thermionic Properties*, edited by G. V. Samonov (Plenum, New York, 1966).

[37]M. A. Melkanoff, T. Sawada, and J. Raynal, *Methods in Computational Physics*, edited by B. Alder, S. Fernbach, M. Rotenberg (Academic, New York, 1966), Vol. 6, p. 11.